Determination of the elastic modulus of mesoporous silica thin films by x-ray reflectivity via the capillary condensation of water

Sandrine Dourdain, D. Britton, H. Reichert, Alain Gibaud

Determination of the elastic modulus of mesoporous silica thin films by x-ray reflectivity via the capillary condensation of water

S. Dourdain,[1,a)] D. T. Britton,[2] H. Reichert,[3] and A. Gibaud[4]

[1]*Structure et Propriété des Architectures moléculaires, UMR 5819, CEA Grenoble, France*
[2]*University of Cape Town, Private Bag Rondebosch 7701, South Africa*
[3]*Max-Planck-Institut für Metallforschung, Heisenbergstraße 3, D-70569 Stuttgart, Germany*
[4]*Laboratoire de Physique de l'Etat Condensé, UMR CNRS 6087, Université du Maine,
72085 Le Mans, France*

The mechanical properties of mesoporous silica films were characterized by x-ray reflectivity measurements. The measurements provide information on the deformation of the pores and the walls induced by the adsorption of water in the pores. The analysis of the nanoscaled deformations supplies a method to determine the elastic modulus E of thin porous films. The nanodeformation of the porous network during its filling with water is interpreted in three regimes of isotherm sorptions. © 2008 American Institute of Physics. [DOI: 10.1063/1.2996412]

Studies of mesostructured hybrid oxide materials carried out on powder samples[1] have shown that the surfactant removal yields mesoporous materials of organized and tailored porosity. In the past years, much effort has been put in the design of thin films of such materials and in the characterization of their structure and physical properties. Fabrication of porous materials in thin films is of great importance for many applications such as low-k dielectrics for electronics,[2] optically active layers,[3] or solar cells with high efficiency derived from mesoporous titania layers.[4] While the design of highly crystalline thin films is nowadays well mastered by a number of groups, the characterization of the mechanical properties of such films remains so far rather difficult.

Methods for the precise measurement of such properties in films as thin as 100 nm are therefore not well established, in contrast to the straightforward determination of for, e.g., the elastic modulus of bulk materials. So far, nanoindentation,[5] surface acoustic waves spectroscopy,[6] or Brillouin light scattering[7] have been employed. While nanoindentation employing the tip of an atomic force microscope is the most frequently used technique, it usually results in overestimated values due to the influence of the substrate. The elastic modulus can be determined if the deformation induced by a given stress is known. We therefore propose to apply a known stress to the film and measure its deformation at a microscopic level. At a more macroscopic level, Mogilnikov *et al.* employed ellipsometry to follow the very small change in the total thickness of porous thin films during capillary condensation and thus derived the elastic modulus.[8] The same method was later employed on organized mesoporous thin films by Boissière *et al.*[9]

In this letter, we describe a microscopic approach where we take advantage of the deformations induced by the capillary condensation of water inside a network of highly organized pores. The nanodeformation of the pores was monitored in situ by the x-ray reflectivity (XRR) technique, which is normally used to access structural properties of very thin porous films.[10,11] We demonstrate that XRR can be used to characterize the mechanical deformations of mesoporous thin films, provided the films are highly organized. This method, based on the direct deformation of the mesopores and walls during the capillary condensation of water, allows, moreover, to interpret the nanoscaled deformations induced at each step of the adsorption of water in the porous network.

Mesoporous silica thin films were synthesized by dip coating a silicon wafer in an initial solution prepared in two steps, following a procedure previously reported.[11,12] A prehydrolyzed solution was first prepared by refluxing for 1 h tetraethoxysilane (TEOS), millipore water, and hydrochloric acid. A second solution, prepared by dissolving the surfactant in ethanol in acidic condition, was then added to the hydrolyzed solution. The film was templated by the surfactant cetyltrimethylammonium bromide (CTAB) with final solutions of respective molar compositions $1TEOS:20C_2H_5OH:0.004HCl:4H_2O:0.10$ and $0.18CTAB$. This composition is known to yield films with a three-dimensional (3D) hexagonal ($P6_3/mmc$) symmetry. This was confirmed by grazing incidence small-angle x-ray scattering.[13] The final sols were aged for 4 days. In order to produce very thin films, the sol was further diluted by adding 21 g of ethanol. The films were subsequently dip coated at a constant withdrawal velocity of 3.6 cm/min on a silicon substrate. The surfactant was finally removed by rinsing the films in a solution containing ethanol and hydrochloric acid with a molar ratio of $1C_2H_5OH: 0.007HCl$ for 1 h and 30 min at $T=60\ °C$.

A cross section of a typical porous structure produced by this procedure is shown in Fig. 1. The highly ordered porous
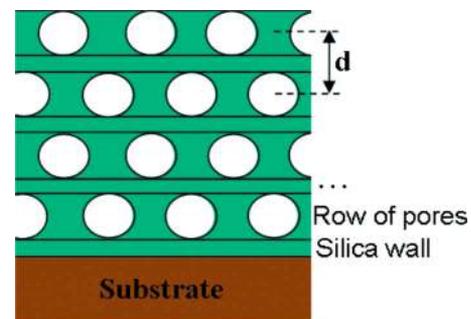

FIG. 1. (Color online) Illustration of a sectional view of a 3D hexagonal mesostructured film. The structure consists of a d-periodic stacking of silica walls and rows of pores in the direction perpendicular to the substrate.
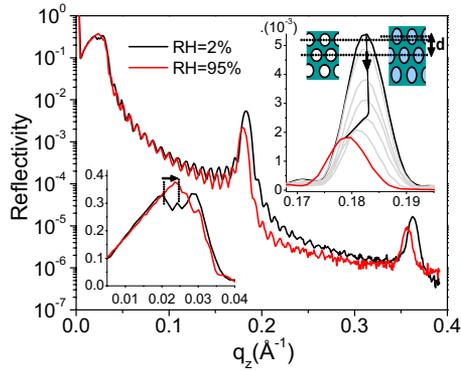
a)Electronic mail: sandrine.dourdain@cea.fr.

FIG. 2. (Color online) XRR of the 3D hexagonal film, measured at RH =2% and RH=95%. The Bragg reflections at 0.18 and 0.37 Å^{-1} originate from the *d*-periodic stacking of pore layers and display changes in intensity and position with increasing filling of the pores with water (upper right inset). The region of total external reflection (lower left inset) shows a shift of the critical angle of total external reflection (marked by the arrow).
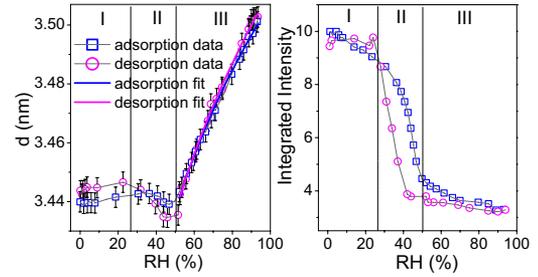

FIG. 3. (Color online) (a) Evolution of the *d*-spacing as a function of the RH during the adsorption and the consecutive desorption of liquid water. (b) Corresponding evolution of the integrated intensity of the Bragg peak, permitting to identify three distinct phases of the isotherm sorption.

film can be considered as a stacking of rows of pores and silica walls in the direction normal to the surface of the films.

Water isotherm sorptions were measured after mounting the samples into a cell adapted to XRR measurements. The relative humidity (RH), defined as the ratio of the partial vapor pressure P of water to the saturation vapor pressure P_0 at ambient temperature, was measured with a humidity sensor HC-610 (Ohmic Instruments). The RH was controlled by flowing either dry or humid nitrogen through the cell. XRR measurements were carried out as a function of RH on a Philips reflectometer using Cu $K\alpha$ radiation at a wavelength of 1.54 Å.

Figure 2 shows XRR of a porous 3D hexagonal film at RH=2% and RH=95%. The differences observed in these two curves clearly highlight the extreme sensitivity of this technique to water condensation inside the pores. The finite thickness of the film produces Kiessig fringes while the periodicity d of the stacking of pores produces Bragg reflections (located at q_z=0.18 and 0.37 Å^{-1}). The total thickness t of the film, determined from the period of the Kiessig fringes, shows that the film swells from t=72 nm at RH =5% to t=73.2 nm at RH=95%. The intensity and location of the Bragg peaks also drastically change upon increasing the RH. At a given RH, their intensity strongly decreases and their position moves closer to the origin of the reciprocal space. These two features are fully consistent with the filling of the pores by water upon capillary condensation. Upon filling the pores with water, the electron density contrast between the matrix and the pores decreases and the Bragg peak intensity thereby decreases. Further increase of the RH induces a swelling of the pores that can be monitored by the shift of the Bragg peaks towards smaller q_z (see upper right inset of Fig. 2). In addition, the critical angle of total external reflection shifts toward higher q_z (see lower left inset of Fig. 2) as a result of the filling of the pores which increases the average electron density of the film.

More subtle details during the adsorption and desorption of water can be derived from monitoring the evolution of the position of the first Bragg peak as a function of RH as shown in the upper right inset of Fig. 2. Upon increasing the RH, the Bragg peak shifts first slightly toward larger q_z-values, before shifting noticeably towards low q_z-values. The corresponding evolution of the *d*-spacing as a function of RH is presented in Fig. 3(a). Figure 3(b) shows the integrated in-

tensity of the Bragg peak during adsorption and desorption cycles. Three regimes of isotherm sorption with a slight hysteresis can be clearly identified.[14] In the following, we summarize the interpretation of the three regimes. Regime I is commonly attributed to the very slow growth of a multimolecular water layer at the mesopores' surface. Regime II corresponds to the onset of capillary condensation during which a fast increase of the water layer occurs. Regime III occurs at high RH when the pores are filled. The three distinct filling regimes correspond to three distinct deformation regimes deduced from the *d*-spacing.

In the low humidity regime I, the *d*-spacing remains constant. The onset of capillary condensation occurs in regime II with a slight decay of the *d*-spacing. Finally, a strong and linear increase of the pore layer spacing d is measured in regime III. The small decrease of d in regime II, has already been observed, but was not interpreted.[8,9] Recently, Ravikovitch and Neimark proposed a molecular simulation by the density functional theory to describe the adsorption induced deformations of micro- and mesoporous materials.[15] They explained and described almost quantitatively nonmonotonic deformations due to molecules adsorption in pores.

In the following, we employ the macroscopic thermodynamics of capillary condensation to propose an interpretation of the three regimes. During the adsorption and desorption of water, the Helmoltz free energy cost dF is mainly related to the surface energy γ between the water droplets and silica. When the surface area of a water droplet changes, the capillary pressure defined by $p_c = P_{\text{liquid}} - P_{\text{vapor}}$, is related to the first derivative of the surface area with respect to the change in volume

$$p_c = \gamma dS/dV = \gamma (dS/dr)/(dV/dr). \qquad (1)$$

This yields, for perfect wetting, to a capillary pressure $p_c = 2\gamma/r$ for a spherical water liquid-vapor interface. Such a behavior is expected in regime III, with a surface tension γ at the water-silica interface.

The regimes I and II are characterized by a different mechanism. The water layer of thickness t grows at the expense of air volume located inside the pores (see Fig. 4).

Changes in the interfacial areas S_{12} and S_{23} are related to the water volume expansion under the pressures $P_1 - P_2$ and $P_2 - P_3$

$$P_1 - P_2 = \gamma dS_{12}/dV \text{ and } P_2 - P_3 = \gamma dS_{23}/dV.$$

Assuming that the radius R of the spherical pore remains almost constant, the capillary pressure inside the pores is given by
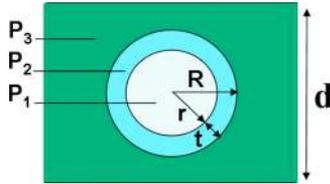
FIG. 4. (Color online) Illustration of the water layer at the surface of the mesopores growing at phases I and II. r is the radius of the convex water liquid-vapor interface, R the radius of the mesopores, and t the thickness of the water layer. P_1, P_2, and P_3 are the pressures of the different phases.

$$P_1 - P_3 = \gamma[(dS_{12} + dS_{23})/dt]/(dV/dt). \tag{2}$$

Using $V = 4/3\pi R^3 - 4/3\pi(R-t)^3$, $S_{12} = 4\pi(R-t)^2$ and $S_{23} = 4\pi R^2$, we find

$$P_1 - P_3 = -2\gamma/(R-t). \tag{3}$$

This relation clearly shows that in the regimes I and II, a negative capillary pressure induces a shrinkage of the film, while in regime III, a positive capillary pressure conversely produces the expansion of the pores filled with water. This agrees very well with the evolution of the d-spacing in regimes II and III. The capillary pressure in the pores is responsible for the contraction and the swelling of the porous network. In regime I, d appears to be constant. In order to explain this discrepancy, the combined deformation of all pores, including the micropores, must be taken into account. The micropores, much smaller than the mesopores, are known to be present in the silica walls.[16] Filled with water (beyond RH = 10%), swelling of the silica walls and collapse of the mesopores occurs at the same time in regime I, thus compensating each other.

In regimes I and II, it is difficult to determine a quantitative relationship between the capillary pressure (which depends on t) and the RH. Therefore we deduce the elastic modulus of the film from the deformation of the pores attributed to the known capillary pressure in regime III.

For our highly organized materials, the capillary pressure induces a strain that can be evaluated by monitoring the d-spacing of the Bragg reflections. The definition of the elastic modulus

$$E = \frac{p_c}{\dfrac{d - d_0}{d_0}} \Rightarrow d = d_0\left(1 + \frac{p_c}{E}\right) \tag{4}$$

yields a linear dependence of the d-spacing with the capillary pressure. In regime III, the capillary pressure p_c is related to the RH via the Kelvin equation

$$\ln(RH) = \frac{p_c V_L}{RT}, \tag{5}$$

where V_L is the molar volume of water, $R = 8.31$ J/K, T is the temperature in Kelvin, and p_c is the capillary pressure. The d-spacing as a function of RH is therefore given by

$$d_{III} = d_0^{III}\left(1 + \frac{RT}{EV_L}\ln RH\right). \tag{6}$$

The experimentally determined d-spacing in regime III is hence fitted as shown in Fig. 3(a). From the slope of the curve d_{III} versus $\ln(RH)$, the elastic modulus is found to be 4.5 ± 0.5 GPa during adsorption and 4.8 ± 0.5 GPa during desorption. The calculated uncertainties take into account the errors in the determination of the pore layer spacing d, the refraction correction, and the errors in T and RH. The values of the elastic modulus are in the same order of magnitude than the values reported for the same kind of materials, using different techniques.[9,17]

Oppositely to the methods previously reported,[8,9] we investigate directly the deformations of the pores and walls size by monitoring the Bragg Peak position. The global swelling of the film could also have been investigated by analysing the Kiessig fringes. However, at high humidity, the increase in total thickness is both due to the swelling of the pores and to a native condensation water layer at the rough top surface of the film. Monitoring the Bragg reflection position enables therefore to attribute exclusively the thickness increase to the swelling of the pores and then to the capillary pressure. Our results demonstrate that the deformation of pores and walls can be measured quantitatively by XRR and yield reliable values for the elastic modulus of films as thin as 100 nm. A key factor is the high degree of organization of the pores in the silica mesoporous structure, such that the evolution of the pore layer spacing d_{III} can be determined with high accuracy as a function of RH.

[1] C. T. Kresge, M. E. Leonowicz, W. J. Roth, J. C. Vartuli, and J. S. Beck, Nature (London) **359**, 710 (1992).

[2] R. Saxena, O. Rodriguez, W. Cho, W. N. Gill, J. L. Plawsky, M. R. Baklanov, and K. P. Mogilkinov, J. Non-Cryst. Solids **349**, 189 (2004).

[3] C. Sanchez, B. Lebeau, F. Chaput, and J.-P. Boilot, Adv. Mater. (Weinheim, Ger.) **15**, 1969 (2003).

[4] M. Zukalova, A. Zukal, L. Kavan, M. K. Nazeeruddin, P. Liska, and M. Grätzel, Nano Lett. **5**, 1789 (2005).

[5] J. L. Hay and G. M. Pharr, *Instrumented Indentation Testing*, ASM Handbook, Mechanical Testing and Evaluation, edited by H. Kuhn and D. Medlin (ASM International, Metals Park, Ohio, 2000), Vol. 8, p. 232.

[6] C. Flannery and C. Murray, Thin Solid Films **338**, 1 (2001).

[7] C. M. Flannery and M. R. Baklanov, *Proceeding of the International Interconnect Technology Conference* (IEEE, New York, 2002), p. 233.

[8] K. P. Mogilnikov and M. R. Baklanov, Electrochem. Solid-State Lett. **5**, F29 (2002).

[9] C. Boissière, D. Grosso, S. Lepoutre, L. Nicole, A. B. Bruneau, and C. Sanchez, Langmuir **21**, 12362 (2005).

[10] A. Gibaud, S. Dourdain, and G. Vignaud, Appl. Surf. Sci. **253**, 3 (2006).

[11] S. Dourdain, J. F. Bardeau, M. Colas, B. Smarsly, A. Mehdi, B. M. Ocko, and A. Gibaud, Appl. Phys. Lett. **86**, 113108 (2005).

[12] S. Dourdain and A. Gibaud, Appl. Phys. Lett. **87**, 223105 (2005).

[13] S. Besson, T. Gacoin, C. Ricolleau, C. Jacquiod, and J. P. Boilot, J. Mater. Chem. **13**, 404 (2003).

[14] K. S. W. Sing, D. H. Evertt, R. A. W. Hual, L. Mocsou, R. A. Pierotti, J. Rouquerol, and T. Siemienievska, Pure Appl. Chem. **57**, 603 (1985).

[15] P. Ravikovitch and A. Neimark, Langmuir **22**, 10864 (2006).

[16] M. Imperor Clerc, P. Davidson, and A. Davidson, J. Am. Chem. Soc. **122**, 11925 (2000).

[17] N. Chemin, M. Klotz, V. Rouessac, A. Ayral, and E. Barthel, Thin Solid Films **495**, 210 (2006).